

## TIME DOMAIN BORN APPROXIMATION

J.H. Rose  
Ames Laboratory, U.S. DoE  
Iowa State University  
Ames, Iowa 50011

J.M. Richardson  
Rockwell International Science Center  
1049 Camino Dos Rios  
Thousand Oaks, California 91360

### ABSTRACT

The time domain Born approximation for ultrasonic scattering from volume flaws in an elastic medium is described. Results are given both for the direct and the inverse problem. The time domain picture leads to simple intuitive formulas which we illustrate by means of several simple examples. Particular emphasis is given to the front surface echo and its use in reconstructing the properties of the flaw.

### INTRODUCTION

Much of the recent development of ultrasonics for quantitative nondestructive engineering (NDE) applications has been due to the close interaction of both theory and experiment. One small difficulty in this situation is as follows. Most of the experiments are performed using a pulsed transducer with a consequent wide band of frequencies. The data is collected as time domain records and may be thought of as the impulse response function of the flaw convolved with the transducer's pulse shape. On the other hand, most of the theory for elastic wave scattering has been calculated in terms of the wavevector  $\vec{k}$  of an incident plane wave. The result is a certain mismatch in the comparison of theory with experiment.

The weak scattering limit yields one of the simplest theories of elastic wave scattering. For cases of interest to NDE, this limit was studied systematically by Gubernatis et al,<sup>1</sup> in terms of the Born approximation.<sup>2</sup> Their work was carried out in the wavevector (or frequency) domain and considerable intuitive understanding of the problem resulted. Despite its simplicity, the frequency domain Born approximation has been widely useful in systematizing experimental data. Further, it has led to the development of a rather successful inversion scheme.<sup>3</sup> Recently, the authors have formulated the weak scattering theory in the time domain using the Born approximation.<sup>4</sup> This new formulation is also rich in its own insights and intuitions. The time domain picture gives rise to simple transparent formulas for the scattering problem which allow the solutions of many problems by inspection. The scattering amplitude for more complicated problems can be easily estimated roughly in an intuitive way. Similarly, simple intuitive formulas are obtained for the inverse problem: i.e., determining the shape and the material composition of the flaw from the scattering. It is the purpose of this paper to introduce the NDE community to these new results. Several simple example cases are treated in order to illustrate the straightforward and useful nature of the formulas. The details of the mathematical derivation will be reserved for a forthcoming paper in which we present a time domain integral equation approach. The Born approx-

imation is obtained as the first iteration of this integral equation.

Before proceeding we remind the reader of the practical limitations of the Born approximation for the direct problem. The Born approximation is a weak scattering theory. Good results will be obtained for a finite flaw, in other than the forward scattering direction, if the material parameters of the flaw are sufficiently close to those of the host. However, the approximation is surprisingly robust and useful results have been obtained for a wide class of flaws, including voids. Often in NDE application, the flaws scatter the ultrasound strongly. In such cases, the frequency domain Born approximation yields its best results for lower frequencies and for directly back scattered signals.<sup>1</sup> At high frequencies the Born approximation fails for forward scattering. In the time domain, we expect the back scattered early arriving signal to be best described. Later arriving signals will tend to involve possible multiple reflections which are ignored in the Born approximation.

The Born approximation has been shown to yield an exact inverse method for the shape and material parameters for the weak scattering flaws described above.<sup>5</sup> Further, it has been successful, in several empirical tests, in the determination of the shape and size of strongly scattering flaws such as spheroidal voids.<sup>3,6,7</sup> Recently, the authors have shown that the inverse Born approximation leads to an exact determination of the shape of an ellipsoidal void in an isotropic elastic solid given ideal data for the scattering amplitudes (i.e., precise longitudinal to longitudinal (L+L) pulse-echo data at all frequencies, and for all angles of incidence).<sup>8</sup> These results are most easily elucidated in the time domain and are the subject of a forthcoming paper. The present form of the Born inverse scattering theory has not been tested for crack-like defects or multiple flaws.

The purpose of this paper is to illustrate the use of the time domain Born approximation for the simple case of finite sized volume inclusions with constant material parameters. In keeping with our limited purposes, we consider primarily longitudinal to longitudinal (L+L) scattering. In Section II, we summarize the formulas for the

determination of the impulse response function. Section III illustrates the use of these formulas for two simple flaws. Section IV summarizes the formulas for the inverse scattering problem. Results are discussed both for the determination of the shape and the material parameters of flaws. We also comment on the applicability of these methods for strongly scattering flaws. In Section V we illustrate the use of the inverse scattering method for a spherical flaw. Section VI is a brief conclusion. The appendix gives formulas for the impulse response functions for  $L \rightarrow L$ ,  $L \rightarrow T$ ,  $T \rightarrow L$ , and  $T \rightarrow T$  scattering from inhomogeneous isotropic flaws with various polarizations of  $T$  (transverse) waves.

#### TIME DOMAIN SCATTERING FORMULAS

Consider an isotropic homogeneous inclusion with material parameter  $\rho_F, \lambda_F$  and  $\mu_F$  embedded in an isotropic homogeneous host material with constant material parameters  $\rho_0, \lambda_0$  and  $\mu_0$ . Here  $\rho$  is the density and  $\lambda$  and  $\mu$  are the Lamé parameters. The deviations of the flaws material parameters are defined as  $\delta\rho = \rho_F - \rho_0$ ,  $\delta\mu = \mu_F - \mu_0$  and  $\delta\lambda = \lambda_F - \lambda_0$ . In order to describe the scattering we consider a longitudinally polarized impulse incident upon the flaw which is centered about the origin of coordinates. The incident impulse is described by

$$\vec{U}_I(\vec{r}, t) = U_0 \delta(t - r/c) \hat{e}_i \quad (1)$$

Here  $\hat{e}_i$  is the direction of incidence,  $c$  is the velocity of longitudinal sound in the host, and  $U_0$  determines the magnitude of the impulse. The amplitude of the scattered displacement field far from the flaw is given in the Born approximation<sup>4</sup> by

$$\vec{U}_S(\vec{r}, t) \xrightarrow{r \rightarrow \infty} \frac{\hat{e}_0}{r^2} f(\hat{e}_i, \hat{e}_0) \frac{1}{c^2} \frac{d^2}{dt^2} \int d^3\vec{r}' \gamma(\vec{r}') \delta(t - \frac{r'}{c} - \frac{\hat{e}_i \cdot \hat{e}_0}{c} \cdot \vec{r}) \quad (2)$$

Here  $\hat{e}_0$  denotes the direction of scattering. The characteristic function,  $\gamma$ , is one inside the flaw and is zero outside. Hence, it defines the flaw's shape. The function  $f(\hat{e}_i, \hat{e}_0)$  depends only on the relative angle between  $\hat{e}_i$  and  $\hat{e}_0$  and is given by

$$f(\hat{e}_i, \hat{e}_0) = \frac{1}{4\pi} \left[ \frac{\delta\rho}{\rho_0} \hat{e}_i \cdot \hat{e}_0 - \frac{\delta\lambda + 2\delta\mu(\hat{e}_i \cdot \hat{e}_0)^2}{\lambda_0 + 2\mu_0} \right] \quad (3)$$

Eq. (2) is still somewhat clumsy for describing the displacement field since it depends explicitly on the position and time at which the signal is measured. We obtain an expression which is independent of  $r'$  and  $t'$  by the transformation

$$\vec{R}(t, \hat{e}_i, \hat{e}_0) = \hat{e}_0 r' \vec{U}_S(\vec{r}', t)/U_0 \quad (4a)$$

$$\vec{R}(t, \hat{e}_i, \hat{e}_0) = f(\hat{e}_i, \hat{e}_0) \hat{e}_0 \frac{1}{c^2} \frac{d^2}{dt^2} \int d^3\vec{r}' \gamma(\vec{r}') \delta(t - (\hat{e}_i - \hat{e}_0) \cdot \vec{r}'/c) \quad (4b)$$

Here we have set  $t = t' - r'/c$ . The origin of time is defined by Eq. (1) and corresponds to the unimpeded incident pulse (Eq. 1) crossing the origin of coordinates. Further, we have normalized  $U_S$  by  $r'$  and  $U_0$  to obtain a quantity,  $\vec{R}$ , which does not depend either on the intensity of the incident pulse or on the distance at which the asymptotic scattering is measured.  $\vec{R}$  is called the impulse response function of the flaw and its expression in Eq. (4) is the basic result of the direct scattering theory.  $\vec{R}$  corresponds to the time domain train of signals which would be received by a transducer in the scattering direction  $\hat{e}_0$  due to an incident delta function displacement pulse in the incident direction  $\hat{e}_i$ .

There are two important observations to be made about  $\vec{R}(t, \hat{e}_i, \hat{e}_0)$ . First, it is the Fourier transform of the  $L \rightarrow L$  scattering amplitude,  $\vec{S}$ , in the  $k$ -domain.<sup>4</sup>  $\vec{S}$  is defined by the asymptotic scattered displacement field

$$\vec{U}_S(|\vec{k}|, \hat{e}_i, \hat{e}_0) \xrightarrow{r \rightarrow \infty} \vec{S}(|\vec{k}|, \hat{e}_i, \hat{e}_0) e^{ikr}/r \quad (5)$$

Then  $\vec{R}$  is determined by

$$\vec{R}(t, \hat{e}_i, \hat{e}_0) = \frac{1}{2\pi} \int_{-\infty}^{\infty} d\omega \vec{S}(\omega/c, \hat{e}_i, \hat{e}_0) e^{-i\omega t} \quad (6)$$

where we have the relation  $\omega = ck$ .

The second important observation is a simple geometrical interpretation of  $\vec{R}$ . First we note that  $f$  depends only on the angle between the incoming and outgoing wave. The integral in Eq. (4b) corresponds to the cross-sectional area,  $A(t)$ , of the flaw evaluated on a plane defined by

$$\vec{r} \cdot (\hat{e}_i - \hat{e}_0) = ct \quad (7)$$

This plane defines the locus of points in the flaw which have a constant travel time from the initiating transducer to the receiving transducer. The simple planar form of this locus results from the weak scattering assumption that the incident impulse travels at the velocity of the host inside the flaw and that the signal is determined by single scattering events. Figure 1 illustrates the geometrical interpretation of  $A$  for a given incident and exit direction. The time dependence of the scattering from quite complicated shapes is now straightforward and a great deal can be learned simply by inspection.

#### EXAMPLES OF THE DIRECT SCATTERING PROBLEM

The use of the time domain Born approximation to determine the impulse response function is illustrated below for two simple flaws. First, scattering from a cubical flaw is used to illustrate pulse-echo calculations. By altering the incident direction such that the incoming impulse

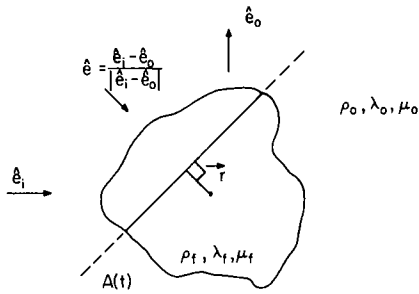


Fig. 1 Shows the geometric interpretation of time domain scattering. The impulse response function is proportional to  $A''(t)$ .  $A(t)$  is defined as the cross-sectional area of the flaw perpendicular to  $r$ ; and  $t \approx (e_i - e_o) \cdot r/c$ .

first contacts on a face, on an edge or on a point, we illustrate several different characteristic forms for  $\tilde{R}(t, \hat{e}_i, \hat{e}_o)$ . Of particular interest, we have included a case in which the front surface echo has no outstanding features and might "disappear" in an experimental measurement. Our second illustration shows the determination of  $\tilde{R}(t, \hat{e}_i, \hat{e}_o)$  for pitch-catch scattering from a sphere.

The impulse function is conveniently expressed for computational purposes after a change of variable, namely  $s = ct/|e_i - e_o|$ . Rewriting Eq. (4)

$$\tilde{R}(s, \hat{e}_i, \hat{e}_o) = \frac{\hat{e}_o f(\hat{e}_i, \hat{e}_o) c}{|\hat{e}_i - \hat{e}_o|} \frac{d^2}{ds^2} \int d^3r \gamma(\vec{r}) \delta(s - \hat{e} \cdot \vec{r}). \quad (8)$$

Here

$$\hat{e} \equiv (\hat{e}_i - \hat{e}_o)/|\hat{e}_i - \hat{e}_o|.$$

The impulse response function is proportional to the second derivative of the cross-sectional area of the flaw,  $A(s)$ , projected on a plane perpendicular to  $\hat{e}$  and at a distance  $s$  from the center of the coordinate system. For the illustrative cases we choose the origin of coordinates to be the center of inversion symmetry.

The determination of  $\tilde{R}$  reduces to finding  $A''(s)$ . Consider the case when the incident impulse is incident parallel to a cube face.  $A$  and  $A''$  are shown in Fig. 2. Scattering from a cube face is characteristic of scattering from a flat on a flaw surface which lies parallel to the incident impulse. The front surface echo is the derivative of a delta function. Figure 3 shows the impulse response function when the incident impulse is parallel to a cube edge. The result is a front surface echo consisting of a delta function. Finally, and perhaps most surprisingly, we consider the scattering of the incident impulse which initially contacts the cube on one of its corners (the most common situation for a randomly chosen angle of incidence). The result is shown in Fig. 4. Note that the front surface echo shows no singular behavior. This last result is generally

(100)-DIRECTION

SC80-10543

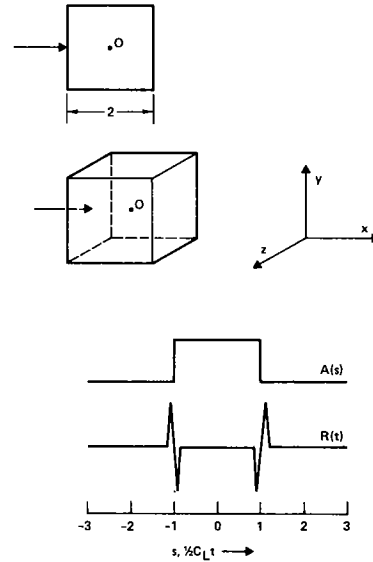


Fig. 2 Pulse-echo scattering from a cube face. The outstanding feature of this result is the appearance of the derivative of a delta function in the front surface echo.

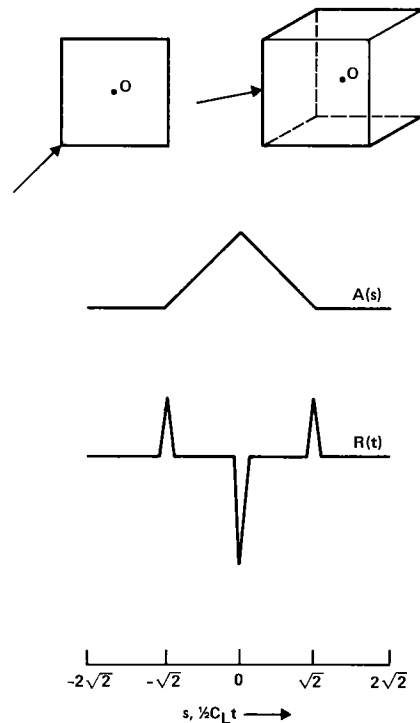


Fig. 3 Impulse response function for pulse-echo scattering from a cube edge. The front surface echo is now a delta function.

true for pulse-echo scattering from the point of a flaw. For these cases the front surface-echo is not notably different from the other parts of the

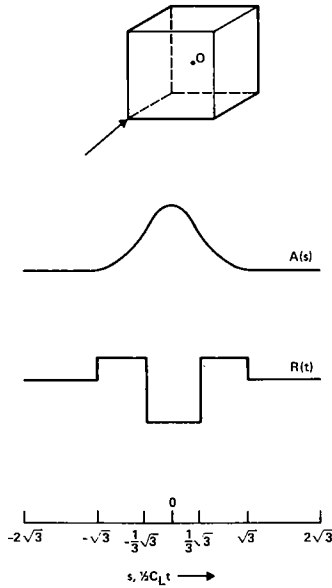


Fig. 4 Impulse response function for pulse-echo scattering from a cube corner. Here there is no singular behavior of the front surface echo.

returning signal. Experimentally, the front surface echo may seem to "disappear." Such a lack of a front surface echo has been observed for star shaped iron flaws in  $S_{i3}N_4$ .<sup>9</sup>

We conclude this section by considering pitch-catch scattering from a spherical flaw. For illustration we have chosen  $e_i$  such that the angle of incidence is  $0^\circ$  and such that the scattering angle is  $120^\circ$ . The resulting  $A(s)$  is on a plane surface perpendicular to the vector  $e = (e_i - e_o) / (|e_i - e_o|)$ . The cross-sectional area of the sphere is given by

$$A(\hat{e}, s) = \pi(R^2 - s^2), \quad |\hat{s}| < R. \quad (9)$$

Here  $R$  is the flaw's radius.  $A$  and its first two derivatives with respect to  $s$  are shown in Fig. 5. The impulse response function is given by

$$\begin{aligned} \hat{R}(\hat{e}_i, \hat{e}_o, s) = & \frac{\hat{e}_o \cdot f(\hat{e}_i, \hat{e}_o) c}{|\hat{e}_i - \hat{e}_o|^3} (2\pi R)^{-1} [\delta(s + R) \\ & + \delta(s - R) - \frac{1}{2} R \theta(R - |s|)] \end{aligned} \quad (10)$$

The appearance of a delta function in the front surface echo is characteristic of scattering from a flaw which has a finite radius of curvature everywhere. Additionally, we note that the substitution  $s = ct/|\hat{e}_i - \hat{e}_o|$  indicates the pulse train will be longest when  $\hat{e}_i = -\hat{e}_o$  (backscatter) and will become progressively shorter as  $\hat{e}_i \rightarrow \hat{e}_o$  (forward scatter). For exactly forward scatter, all of the scattered energy would arrive simultane

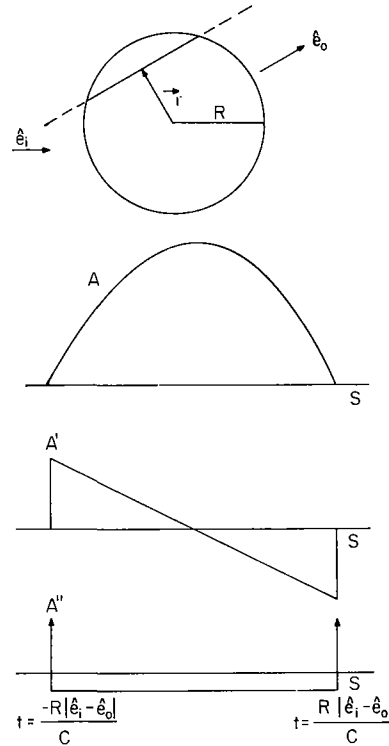


Fig. 5 Pitch-catch scattering from a sphere. Notice that for a flaw with finite radii of curvature the front surface echo is a delta function.

ously with the incident impulse resulting in the high frequency divergence for forward scatter. These results stem from the Born assumption that the velocity of propagation in the flaw is the same as in the host.

#### THE INVERSE SCATTERING PROBLEM

For the class of flaws we are considering, the inverse problem consists of two parts. First, the determination of the flaw's characteristic function (i.e., the shape). Second, the determination of the material parameters. Below we give the formula (valid in the weak scattering limit) for exactly reconstructing the shape of the flaw. Then we show how the specular reflection can be used to deduce the material properties of the flaw. We concentrate on the front surface echo (the specular reflection) since we know that the weak scattering assumption is violated for many of the flaws encountered in practice. We expect that the early arriving specular reflection will be given more accurately by the Born approximation than the later arriving signal. Our expectation is based on the fact that by considering only the first arriving signal we avoid multiple reflections within the flaw. Formulas are given for determining  $\delta\lambda$  and the difference in the acoustic impedance,  $\delta Z$ , in terms of the front surface echo. We also discuss similar results for  $\Delta\rho$  and  $\Delta\mu$ .

which can be obtained from L+T and T+T scattering, respectively.

The shape of a flaw can be determined from L+L pulse-echo data measured for all incident directions,  $\hat{e}_i$ . The characteristic function is determined from the impulse response<sup>4</sup> and is

$$\gamma(\vec{r}) = \text{const.} \int d^2\hat{e}_i R(t = \frac{2\hat{e}_i \cdot \vec{r}}{c}, \hat{e}_i, -\hat{e}_i) . \quad (11)$$

Geometrically, this is equivalent to adding up the backscattered impulse response functions for all angles of incidence,  $\hat{e}_i$ , and for those times,  $t = 2\hat{e}_i \cdot \vec{r}/c$  which include scattering coming from the point  $\vec{r}$ . Equation (11) applies to flaws with spatially variable material parameters if we replace the characteristic function,  $\gamma$ , with the acoustic impedance function  $\delta z(\vec{r})$ . Here  $\delta z(\vec{r}) = \rho_f(\vec{r})c_f(\vec{r}) - \rho_h(\vec{r})c_h(\vec{r})$ , where  $\rho_f(\vec{r})$  and  $\rho_h(\vec{r})$  denote the spatially variable densities of the flaw and the host. Similarly  $c_f(\vec{r})$  and  $c_h(\vec{r})$  indicate the spatially variable longitudinal velocities.

The material properties of the flaw can be extracted from Eq. (4) as follows. The time dependence of the impulse response function is given by the second time derivative of the cross-sectional area function. However, the magnitude of the impulse response function is determined by the angular factor  $f(\hat{e}_i, \hat{e}_0)$ . By choosing special incident and exit directions we can determine the material properties. Consider the case of direct back scattering in which case  $\hat{e}_0 = -\hat{e}_i$ . Then

$$f = -\frac{1}{2\pi} \frac{\delta z}{z_0} . \quad (12)$$

Here  $z_0$  is the acoustic impedance ( $z_0 = \rho_0 c$ ) and  $\delta z$  is the difference in the acoustic impedance of the flaw and the host. Thus, if the acoustic impedance of a flaw is greater than that of the host  $R(t, \hat{e}_i, -\hat{e}_i)$  will be inverted with respect to the incident pulse. On the other hand, if  $\delta z$  is less than zero,  $R$  will be upright.

The Lamé' parameter  $\lambda$  can also be determined from L+L scattering. Here choose  $\hat{e}_0$  to be perpendicular to  $\hat{e}_i$ . Then

$$f = \frac{1}{4\pi} \frac{\delta \lambda}{\lambda + 2\mu} . \quad (13)$$

Similarly,  $\delta \rho$  can be obtained from L+T scattering and for  $\delta \rho$  and  $\delta \mu$  from T+T scattering. Thus by considering L+L and T+T pulse-echo scattering alone, we find the material parameters of the flaw. For weak scattering flaws the magnitude of the signal (and front surface echo) determines  $\Delta \lambda$ ,  $\Delta \rho$  and  $\Delta \mu$  via Eqs. (12) and (13) and their analogs for T+T scattering. For strongly scattering flaws, we do not expect an accurate relation. However, it is possible that by observing the sign of the front surface echo for strongly scattering flaw, we will be able to determine the signs of  $\delta \rho$ ,  $\delta \mu$ ,  $\delta \lambda$  and  $\delta z$ . In this connection it is worthy of note that it was shown by one of us<sup>5</sup> that with a sufficient diversity of pitch-catch L+L scattering measurements one can estimate (in principle) the spatial distribution of  $\delta \rho$ ,  $\delta \lambda$ , and  $\delta \mu$ .

## INVERSE BORN APPROXIMATION FOR THE SHAPE

In order to illustrate the use of the inversion algorithm implied by Eq. (8), we consider the case of a spherically symmetric flaw. Then the time domain inversion algorithm (Eq. 11) reduces to

$$\gamma(|\vec{r}|) = \text{const.} \frac{1}{2r/c} \int_{-2r/c}^{2r/c} R(t, \hat{e}_i, -\hat{e}_i) . \quad (14)$$

Here  $\hat{e}_i$  is arbitrary since the flaw has spherical symmetry. The characteristic function is given by a time domain average of the impulse response function about the zero of time. Using the impulse response function for a sphere, which is shown in Fig. 5, we see that the characteristic function,  $\gamma$ , will be a constant for values of  $r$  less than the radius. For a value of  $r$  equal to the radius,  $\gamma$  will drop discontinuously to zero. Further,  $\gamma$  is zero for  $r$  greater than the radius. Thus we have reconstructed the characteristic function of a sphere. The Born inversion algorithm appears to be much more general than its derivation as a weak scattering limit might suggest. Figure 6 shows the reconstruction of the characteristic function for a spherical void in Ti using the exact scattering results of Ying and Truell.<sup>10</sup>

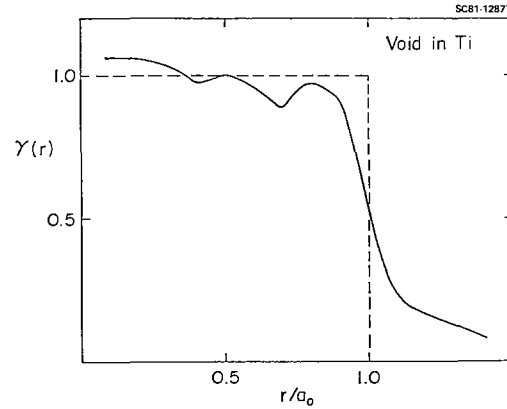


Fig. 6 Calculated characteristic function for a spherical void in Ti using the Inverse Born Approximation.

The inversion algorithm for spherical flaw is significantly simpler to implement than the general form, Eq. (11). It has been found that the simplest form of the inverse Born approximation Eq. (14) can be used to study the shape of ellipsoidal flaws.<sup>3,6,7</sup> In this case, rather than determining the distance from the flaws center to the surface, one determines the distance from the center to the tangent planes to the surface.

In order to implement the inversion formulas, it is necessary to experimentally establish the zero of time, which is defined as the instant the unimpeded impulse would have crossed the center of mass of the flaw. For weakly scattering flaws of arbitrary shape, this zero of time can be determined. For flaws with a center of inversion symmetry, there is a general method for determining the zero of time for arbitrarily strongly scattering flaws. These methods rely upon the low frequency expansion of the scattering amplitude or equivalently the first four moments of the impulse

response function. Details can be found in Refs. 11, 12 and 13. For strongly scattering flaws of general shape (with no center of inversion symmetry), the determination of the zero of time is problematic and the implementation of the inversion algorithm is uncertain.

The time domain Born approximation provides a basis for extending the inversion method suggested by Cook et al.<sup>14</sup> They noted (following Kennaugh and Moffat<sup>15</sup> for the electromagnetic case) that if the time domain pulse-echo scattering response to an incident delta function plane wave is proportional to the second derivative of the cross-sectional area (see Eq. 4b), then the scattering response to a ramp function will yield the cross-sectional area of all sections of the flaw perpendicular to the incident direction. Previously, this inversion method has been justified by the use of the physical optics approximation which is most appropriate for voids and for high frequencies. The time domain Born approximation for the impulse response function indicates the inversion method is also justified for weakly scattering inclusions as pointed out by Cook.<sup>16</sup>

#### SUMMARY

We have illustrated the use of the time domain Born approximation. Simple examples were chosen to demonstrate the utility of the approximation both for the direct and the inverse scattering problems. Of particular interest is the manner in which the front surface echo depends on the geometry of the scatterer. The front surface echo allows us to determine the sign of  $\delta z$  and  $\delta \lambda$  from L+L scattering. L+T scattering allows one to infer  $\delta \rho$ , while T+T scattering lead to a knowledge of both  $\delta \rho$  and  $\delta \mu$ . The time domain Born approximation provides a convenient intuitive picture for discussing both the direct and inverse scattering problems.

#### APPENDIX

##### COMPILATION OF L+L, L+T, T+L AND T+T RESULTS

The direct scattering formulas are listed here for L+L, L+T, T+L, and T+T scattering. Further, the material parameters of the flaw are allowed to vary with position. Since the results are considerably more complicated than the simple case of L+L scattering treated in the main text, we change our notation to a more general form. First, the incident impulse is uniformly chosen to propagate in the +z direction. The asymptotic form of the scattered displacement field is represented

$$r U_i^S(\vec{r}, t) / U_0 \xrightarrow{r \rightarrow \infty} A_i(t - r/c_L) + B_i(t - r/c_T) \quad (A1)$$

Here  $U_0$  is the strength of the incident delta function impulse;  $c_L$  and  $c_T$  are, respectively, the velocity of longitudinal and transverse sound. Tensor notation is adopted to denote the component of the vectors  $\vec{U}$ ,  $\vec{A}$  and  $\vec{B}$ .  $\vec{A}$  represents the longitudinal response due to an arbitrarily polarized impulse. If the impulse itself is longitudinally polarized then  $\vec{A}$  is identical to the function  $\vec{R}(t, \hat{e}_i, \hat{e}_0)$  defined in Section II.  $\vec{B}(t)$  is the transverse response to an arbitrarily polarized impulse.

In order to succinctly state the results we define the unit vectors  $\hat{r}$ ,  $\hat{\theta}$  and  $\hat{\psi}$ , where  $\hat{r}$  is the direction of propagation of the scattered wave.

$$\hat{r} = \hat{x} \sin \theta \cos \psi + \hat{y} \sin \theta \sin \psi + \hat{z} \cos \theta$$

$$\hat{\theta} = \hat{x} \cos \theta \cos \psi + \hat{y} \cos \theta \sin \psi - \hat{z} \sin \theta \quad (A2)$$

$$\hat{\psi} = -\hat{x} \sin \psi + \hat{y} \cos \psi.$$

Here  $\theta$  and  $\psi$  are the polar and azimuthal angles of our spherical coordinate system; and  $\hat{x}$ ,  $\hat{y}$  and  $\hat{z}$  are the unit vectors of the rectangular system. Much of the notation in the appendix is taken from the MSC report of Gubernatis et al, which is an excellent account of the frequency space Born approximation.

First, we consider an incident impulse which is longitudinally polarized (Eq. 1). In what follows  $\hat{e}_i$  is always equal to  $\hat{z}$ , the direction of incidence. Nonetheless, we retain  $\hat{e}_i$  for uniformity of notation.

$$A_i(t) = \frac{\hat{r}_i}{4\pi c_L^2} \frac{d^2}{dt^2} \int d^3\vec{r} \gamma(\vec{r}) \frac{\delta \rho(\vec{r}) \cos \theta}{\rho_0} - \frac{\delta \gamma(\vec{r}) + 2\delta \mu(\vec{r}) \cos \theta}{\lambda_0 + 2\mu_0} \delta t - \frac{(\hat{e}_i - \hat{e}_0) \cdot \vec{r}}{c_L} \quad (A3)$$

and

$$B_i(t) = \frac{\hat{\theta}_i}{4\pi c_T^2} \frac{d^2}{dt^2} \int d^3\vec{r} \gamma(\vec{r}) \frac{c_T}{c_L} \frac{\delta \mu(\vec{r})}{\mu_0} \sin(2\theta) - \frac{\delta \rho(\vec{r})}{\rho_0} \sin(\theta) \delta t - \frac{\hat{e}_i}{c_L} - \frac{\hat{e}_0}{c_T} \cdot \vec{r} \quad (A4)$$

Now consider an incident impulse transversely polarized in the +x axis. Then

$$A_i(t) = \frac{\hat{r}_i}{4\pi c_L^2} \frac{d^2}{dt^2} \int d^3\vec{r} \gamma(\vec{r}) \frac{\delta \rho(\vec{r})}{\rho_0} \sin \theta \cos \psi - \frac{\delta \mu(\vec{r})}{\lambda_0 + 2\mu_0} \frac{c_L}{c_T} \sin \theta \cos \psi \delta t - \frac{\hat{e}_i}{c_T} - \frac{\hat{e}_0}{c_L} \cdot \vec{r} \quad (A5)$$

and

$$B_i(t) = \frac{1}{4\pi c_T^2} \frac{d^2}{dt^2} \int d^3\vec{r} \gamma(\vec{r}) \frac{\delta \rho(\vec{r}) \sin \psi}{\rho_0} + \frac{\delta \mu(\vec{r}) \sin \psi \cos \theta}{\mu_0} \hat{\psi}_i + \frac{(\delta \rho(\vec{r}) \cos \theta \cos \psi)}{\rho_0} \hat{\psi}_i + \frac{\delta \mu(\vec{r}) \cos 2\theta \cos \psi}{\mu_0} \hat{\theta}_i \delta t - \frac{\hat{e}_i - \hat{e}_0}{c_T} \cdot \vec{r} \quad (A6)$$

The third case considered is an incident impulse which is right hand circularly polarized. That is

$$U_{+} = U_0 \frac{(\hat{x} + i\hat{y})}{\sqrt{2}} \delta t - \frac{\hat{z} \cdot \vec{r}}{c_T} \quad (A7)$$

we define

$$\begin{aligned} \hat{x}^{+} &= \frac{1}{\sqrt{2}} (\hat{\theta} + i\hat{\psi}) \\ \hat{x}^{-} &= \frac{1}{\sqrt{2}} (\hat{\theta} - i\hat{\psi}) \end{aligned} \quad (A8)$$

then

$$\begin{aligned} A_i(t) &= \frac{e^{i\psi}}{4\pi c_L^2} \frac{d^2}{dt^2} \int d^3r \gamma(\vec{r}) \frac{\delta \rho(\vec{r})}{\rho_0} \\ &\quad - \frac{c_L}{c_T} \frac{\delta \mu(\vec{r})}{\lambda_0 + 2\mu_0} \sin 2\theta \delta t - \frac{\hat{e}_i}{c_L} - \frac{\hat{e}_0}{c_T} \cdot \vec{r} \end{aligned} \quad (A9)$$

Finally

$$\begin{aligned} B_i(t) &= \frac{e^{i\psi}}{4\pi c_T^2} \frac{d^2}{dt^2} \int d^3r \gamma(\vec{r}) \\ &\quad \hat{x}_i^{+} \frac{\delta \rho(\vec{r})}{\rho_0} \frac{(1 + \cos\theta)}{2} - \frac{\delta \mu(\vec{r})}{\mu_0} \frac{\cos\theta + \cos(2\theta)}{2} + \\ &\quad \hat{x}_i^{-} \frac{\delta \rho(\vec{r})}{\rho_0} \frac{\cos\theta - 1}{2} + \frac{\delta \mu(\vec{r})}{\mu_0} \frac{\cos\theta - \cos 2\theta}{2} \\ &\quad \delta t - \frac{\hat{e}_i - \hat{e}_0}{c_T} \end{aligned} \quad (A10)$$

#### ACKNOWLEDGMENT

This work was sponsored by the Center for Advanced NDE operated by the Science Center, Rockwell International, for the Advanced Research Projects Agency and the Air Force Materials Laboratory under Contract No. F33615-80-C-5004.

#### REFERENCES

1. J.E. Gubernatis, E. Domany, J.A. Krumhansl and M. Huberman, Material Science Center, Cornell University, Technical Report 2654 (1975); and J.E. Gubernatis, E. Domany, J.A. Krumhansl: J. Appl. Phys. 48, 2804 (1977).
2. A.K. Mal and L. Knopoff, J. Inst. Math. Applics. 3, 376 (1967).
3. J.H. Rose and J.A. Krumhansl, J. Appl. Phys. 50, 2951 (1979).
4. J.M. Richardson and J.H. Rose, to be published.
5. J.M. Richardson, Proc. of the Ultrasonics Symposium, eds. by J. deKlerk and B.R. McAvoy, 356 (1979).
6. R.K. Elsley and R.C. Addison, Proceedings of the DARPA/AMFL, Review of Progress in Quantitative NDE, 6th Annual Report, in press.
7. J.H. Rose, V.V. Varadan, V.K. Varadan, R.K. Elsley and B.R. Tittmann, Acoustics Electro-magnetic and Elastic Wave Scattering-Focused on the T-Matrix Approach, eds. V.K. Varadan and V.V. Varadan, pub. by Pergamon Press, 605 (1980).
8. J. H. Rose and J. M. Richardson, to be published.
9. L. A. Ahlberg, R. K. Elsley, L. J. Graham, and J. M. Richardson, Proc. of the 1979 Ultrasonics Symposium, 79 CH 1482 - 9, pp. 321-326.
10. C. F. Ying and R. Truell, J. Appl. Phys. 27, 1086 (1956).
11. J.M. Richardson, to be published.
12. J.M. Richardson and R.K. Elsley, "Extraction of Low Frequency Properties from Scattering Measurement," Proceedings of the 1979 IEEE Ultrasonic Symposium, 79CH1482-9, pp. 336-341.
13. J.M. Richardson and R.K. Elsley, "Semi-Adaptive Approach to the Extraction of Low-Frequency Properties from Scattering Measurements," Proceedings of the 1980 IEEE Ultrasonic Symposium, 80CH1602-2, pp. 847-851.
14. B.D. Cook, S. Wilson and R.L. McKinney, Proceedings of the DARPA/AMFL Review of Progress in Quantitative NDE, 6th Annual Report, in press.
15. E.N. Kennaugh and D.L. Moffat, Proc. IEEE, 53, 893 (1965).
16. B.D. Cook, private communication.